

Xenia: A Probe of Cosmic Chemical Evolution

Summary

Metals are essential for star formation and the subsequent evolution of stars, and ultimately the formation of planets and the development of life. Reconstructing the cosmic history of metals, from the first population of stars to the processes involved in the formation of galaxies and clusters of galaxies, is a key observational challenge. Most baryons reside in diffuse structures, in (proto)-galaxies and clusters of galaxies, and are predicted to trace the vast filamentary structures created by the ubiquitous Dark Matter. X-ray spectroscopy of diffuse matter has the unique capability of simultaneously probing a broad range of elements (C through Fe) in all their ionization stages and all binding states (atomic, molecular, and solid), and thus provides a model-independent survey of the metals. A medium-size mission, *Xenia* – named for the Greek word for hospitality – will combine cryogenic imaging spectrometers and wide field X-ray optics with fast re-pointing to address *IXO* objectives 3 & 4 from Table 1 of NNH11ZDA018L.

Submitted by:

C. Kouveliotou¹, (256) 961 7604, NASA/MSFC, chryssa.kouveliotou@nasa.gov,

L. Piro², J-W. den Herder³, T. Ohashi⁴, D. Hartmann⁵, D. Burrows⁶, T. Abel⁷, L. Amati⁸, S. Barthelmy⁹, J. Beacom¹⁰, J. Bloom¹¹, M. Bonamente¹², E. Branchini¹³, G. Branduardi-Raymont¹⁴, J. Bregman¹⁵, V. Bromm¹⁶, A. Burkert¹⁷, S. Campana¹⁸, C. Carilli¹⁹, R. Cen²⁰, P. Coppi²¹, C. Danforth²², P. de Korte³, R. Diehl²³, S. Etori⁸, A. Falcone⁶, M. Fall²⁴, X. Fan²⁵, B. Fields²⁶, C. Jones²⁷, G. Ghisellini¹⁸, M. Galeazzi²⁸, N. Gehrels⁹, G. Ghirlanda¹⁸, J. Grindlay²⁷, A. Heger²⁹, P. Henry³⁰, W. Hermsen³, A. Holland³¹, J. Hughes³², K. Irwin³³, J. Kaastra³, H. Kawahara³⁴, N. Kawai³⁵, B. Keel³⁶, R. Kelley⁹, C. Kilbourne⁹, M. Kippen³⁷, A. Kusenko³⁸, A. Loeb²⁷, F. Matteucci³⁹, G. Mathews⁴⁰, P. Meszaros⁶, T. Mineo⁴¹, K. Mitsuda⁴², S. Molendi¹⁸, L. Natalucci², K. Nomoto³³, P. O'Brien⁴³, S. O'Dell¹, F. Paerels⁴⁴, G. Pareschi¹⁸, V. Petrosian⁷, N. Prantzos⁴⁵, J. Primack⁴⁶, X. Prochaska⁴⁶, E. Ramirez-Ruiz⁴⁶, B. Ramsey¹, A. Rasmussen⁷, S. Sasaki⁴, S. Savaglio²³, J. Schaye⁴⁷, S. Snowden⁹, V. Springel⁴⁸, Y. Suto³³, G. Tagliaferri¹⁸, Y. Takei⁴³, Y. Tawara⁴⁹, F. Timmes⁵⁰, L. Townsley⁶, P. Ubertini², A. van der Horst⁵¹, J. Vink⁵², M. Weisskopf¹, R. Wijers⁵¹, S. Woosley⁴⁶, N. Yamasaki⁴³

¹NASA/MSFC, ²INAF-Rome, ³SRON, ⁴Tokyo Metropolitan University, ⁵Clemson University, ⁶Penn State University, ⁷Stanford University, ⁸INAF-Bologna, ⁹NASA/GSFC, ¹⁰Ohio State University, ¹¹UCB, ¹²UA-Huntsville, ¹³Roma Tre University, ¹⁴MSSL, ¹⁵University of Michigan, ¹⁶University of Texas, ¹⁷University of Munich, ¹⁸INAF-Milano, ¹⁹NRAO, ²⁰Princeton University, ²¹Yale University, ²²University of Colorado, ²³MPE, ²⁴STScI, ²⁵University of Arizona, ²⁶UIUC, ²⁷Harvard/SAO, ²⁸University of Miami, ²⁹University of Minnesota, ³⁰University of Hawaii, ³¹Open University, ³²Rutgers University, ³³NIST/Boulder, ³⁴University of Tokyo, ³⁵Tokyo Institute of Technology, ³⁶UA-Tuscaloosa, ³⁷LANL, ³⁸UCLA, ³⁹INAF-Trieste, ⁴⁰University of Notre Dame, ⁴¹INAF-Palermo, ⁴²JAXA/ISAS, ⁴³University of Leicester, ⁴⁴Columbia University, ⁴⁵IAP Paris, ⁴⁶UCSC, ⁴⁷Leiden University, ⁴⁸MPA, ⁴⁹Nagoya University, ⁵⁰Arizona State University, ⁵¹University of Amsterdam, ⁵²Utrecht University

Xenia Website: <http://sms.msfc.nasa.gov/xenia/>

Xenia Video for General Public: <http://www.youtube.com/watch?v=E3SCn3HgXp8>

White Paper by Hartmann et al. 2009: <http://sms.msfc.nasa.gov/xenia/>

Xenia: A probe of Cosmic Chemical Evolution

The study of cosmic structures that grew from initial density perturbations is a frontier of modern observational cosmology. At high redshift the earliest massive stars and their explosions drive the cycle of chemical enrichment. Tomography of the structured Universe with bright background light sources, such as quasars and Gamma Ray Bursts (GRBs), probes the large-scale distribution and physical state of the gas, which is coupled dynamically to the stars and dark matter underlying the basic building blocks of the Universe. In the local Universe, many of the baryons are currently unaccounted for (e.g., [1]), and may reside in a warm-hot tenuous gas that traces the underlying large-scale structures. Understanding cosmic chemical evolution requires sensitive UV and X-ray studies of the diffuse baryons inside galaxy clusters and in the cosmic web that stretches between galaxy clusters and super-clusters (e.g., [2]). The dark side of the Universe and its luminous tracers are coupled, and probing the links between these components will lead to a better understanding of how the Universe transitioned from the dark ages to the rich structures of the present. The *Xenia* mission proposed here will use X-ray monitoring, fast repointing to bright sources, wide field imaging, and high-resolution spectroscopy in a low background environment to map the build-up of cosmic structures on various scales from the high- z Universe to the present time (stars, galaxies and the cosmic web), with emphasis on the distribution and state of the baryonic component (*IXO* objectives 3 & 4 from Table 1 of NNH11ZDA018L).

Xenia will map out the evolution of the metallicity from $z=0$ to $z>6$ using three major tracers: 1) GRBs in (proto)-galaxies, 2) Galaxy Clusters, and 3) the filamentary WHIM. These tracers unfold the chemo-thermo-dynamical history of the ubiquitous diffuse baryons that reside in the Inter-Galactic Medium (IGM), in clusters (the Intra-Cluster Medium, ICM) and inside galaxies (the Interstellar Medium, ISM) and shed light on feedback processes at work in the cosmic multi-component fluid (e.g., [3]; [4]).

Our team is willing to present the *Xenia* concept at the workshop (if invited). We are also willing to discuss any sensitive information with NASA, provided proper arrangements are made to protect any proprietary information.

IXO Objective 3: How does large-scale structure evolve?

(i) Find and characterize the missing baryons by performing high resolution absorption line spectroscopy of the WHIM over many lines of sight:

Cosmological hydrodynamical simulations suggest that the missing baryons in the $z=0-3$ range can be accounted for by a diffuse, highly ionized WHIM, preferentially distributed in large-scale filaments connecting galaxy clusters. This gas is extremely hard to detect: a small fraction may have been revealed through OVI lines but its bulk resides in structures with $T > 10^6$ K. The thermal continuum emission from this hot gas is much too faint to be detectable against overwhelming backgrounds. The only characteristic radiation from this medium is in the discrete transitions of highly ionized C, N, O, Ne, and possibly Fe. At $T \geq 10^{5.5}$ K, *the primary tracers (O VII, O VIII) are only detectable in the soft X-ray regime*. *Xenia* will have sufficient line sensitivity and energy resolution to measure gas densities down to 10^{-5} cm^{-3} , ~ 30 times smaller than currently probed in clusters. ***Xenia can detect these WHIM lines in emission, and in absorption.***

GRBs are beacons illuminating cosmic chemical evolution from the pre-galactic phase of the Universe to the large-scale structures of the present. They are tracers of

the buildup of heavy elements and therefore of the cosmic conversion history of gas into stars. GRBs are ideally suited for this task because: a) their intrinsic spectra are simple, making line modeling straightforward, b) unlike QSOs, they have not altered their environments over large distances and over long periods of time, and c) they are most common from $z \sim 1-3$. The X-ray band offers a powerful tool for these studies, as essentially all GRBs are followed by bright X-ray emission. Afterglows fade fast, thus requiring a rapid repointing capability, which, coupled with the high-resolution soft X-ray spectroscopy of the *Cryogenic Imaging Spectrometer (CRIS)* will open a new window on the WHIM studies. Figure 1 (from [4]) shows the power of GRB X-ray spectroscopy with *Xenia*. The *Xenia Transient Event Detector (TED)* will ensure a high GRB detection rate, providing a 5-year sample of 400 afterglows with 50 ks high-resolution spectroscopic observations. Of these about 180 with fluence $> 2 \times 10^{-6}$ will be used to study the WHIM (see Table 1).

Figure 2 shows simulations of a typical CRIS mapping observation of a $\sim 4^\circ$ field, which encompasses the typical scale of the filaments and enables 3D probing of the large-scale structure of the WHIM [5]. We modeled the properties of the WHIM with large scale Dark Matter + hydrodynamic simulations, with a parameterized treatment of stellar feedback, using the simulations of [5] and [6] to investigate various WHIM models [4]. Here we focus on a model that includes large scatter in metallicity (see also [7]). This model reproduces the observed properties of the intergalactic OVI absorbers (e.g. [8]), and is based on a phenomenological treatment of the physical distribution and state of the intergalactic metals, including the effects of feedback and departures from thermal equilibrium. These simulations show that *CRIS* will obtain ~ 200 combined 5σ detections of O VII and O VIII resonance absorption lines from the WHIM in 50 ks observations of the brightest ~ 180 GRBs (Table 1). A third of these systems will be probed in emission through deeper observations as the GRB fades, providing a unique opportunity to measure the intergalactic absorption with high statistics and to characterize the physical state (temperature, density, and metal content) and evolution of the WHIM through emission and absorption measurements along the same lines of sight.

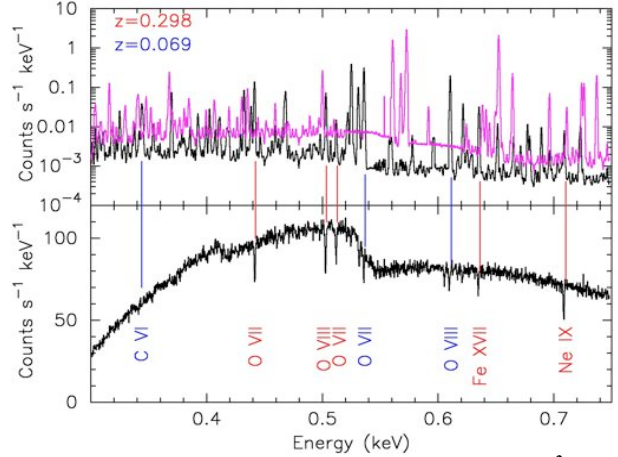


Figure 1: Emission spectrum of a 4 arcmin^2 area (top), and absorption spectrum (bottom) of the same region of the sky, as measured by *Xenia*. In the top panel the emission of two red-shifted components is shown in black, while the emission of the Galactic foreground is shown in purple. In the bottom panel the spectrum of the same systems is shown, but now in absorption using a bright GRB as a beacon. [4]

Table 1: Estimated number of absorption systems detected at $>5\sigma$ per year by *Xenia* [4]

Fluence 0.3-10 keV [erg cm ⁻²]	# GRBs [yr ⁻¹]	EW _{min} O VII [eV]	EW _{min} O VIII [eV]	# O VII/VIII [yr ⁻¹]
$>1 \cdot 10^{-5}$	6	0.12	0.08	19
$>5 \cdot 10^{-6}$	13	0.18	0.12	29
$>2 \cdot 10^{-6}$	36	0.28	0.19	37

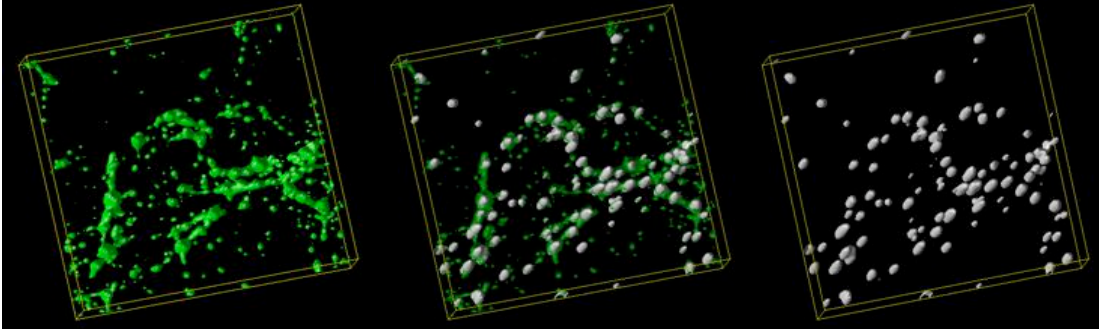


Figure 2: **Left:** Simulation of the 3D distribution of gas in a $4.2^\circ \times 4.2^\circ$ field (~ 50 Mpc on a side) within a narrow redshift slice of $0.202 < z < 0.212$ [9]. **Right:** The white blobs show the gas detected through OVII and OVIII emission lines with significance $> 3\sigma$ each. This structure closely traces the high-density regions of the gas, with only a few spurious detections. **Middle:** Overlay of the left and right panel.

(ii): Measure the growth of cosmic structure and the evolution of the elements by measuring the mass and composition of ~ 500 clusters at $z < 2$

Xenia will map temperatures, masses, and abundances of many clusters beyond the virial radii using CRIS and a *High Angular Resolution Imager (HARI)*, and will study their evolution to their formation epochs beyond $z \sim 1$ (Figure 3). X-ray mapping beyond the virial radii is essential for determining the mass and emission profiles of clusters, and to trace the connection between the cluster gas and the WHIM in the outer cluster regions. Cen & Ostriker [9] were the first to investigate the properties of these WHIM-filled structures, and found that at “low- z ” ($z < 2$) about half of all baryons are expected to reside in the filaments connecting galaxy clusters, and their hydrogen densities should be $< 10^{-4} \text{ cm}^{-3}$, with temperatures in the range $10^5 - 10^7 \text{ K}$. *This parameter range is not conducive to easy detection.* Still, detections were reported in recent years, albeit with low statistical significance and lack of independent confirmation. *XMM-Newton* observations [10] of the cluster pair Abell 222/223 ($z=0.2$), confirmed the presence of an X-ray emitting inter-cluster bridge (a filament) with conditions expected from simulations [11], offering impetus to advanced studies with significantly more sensitive instrumentation. The frontier in this field is the ability to map cluster mass, temperature, and metal abundances to significantly larger radii (lower overdensities), so the transition from the intra-cluster gas to the connecting cosmic web can be explored. *Xenia* will provide the crucial extension of X-ray imaging and spectroscopy from the inner to the outer parts of clusters (Figure 3), and thereby connect to the issue of the missing baryons in the WHIM.

Deep surveys using *Xenia*’s wide FoV will allow detailed studies of cluster evolution to their formation epochs ($z > 1$), and will enable firm detections of WHIM emission in areas of significantly lower cosmic overdensities ([12]; [2]), which will aid investigations of the role of feedback mechanisms (e.g., [13]). Detection of isolated inter-cluster filaments with low overdensities requires a combination of sensitive instruments and long observation times. *Xenia* is well suited for this task in view of its low background (low earth orbit) combined with a constant angular resolution over a large field of view, which enables homogeneous and efficient mapping of spatially extended structures.

IXO Objective 4: What is the connection between SMBH formation and evolution of large-scale structure (i.e., cosmic feedback)? Measure metallicity and velocity of hot gas in galaxies and clusters

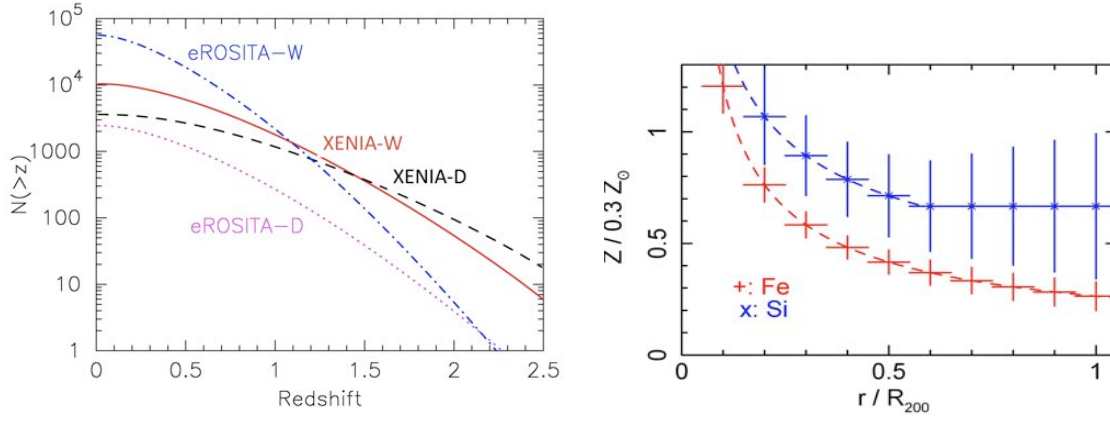


Figure 3: **Left:** Comparison between the number of clusters seen by Xenia and by eROSITA Wide and Deep surveys as a function of redshift. **Right:** Abundance model profiles (solid lines) from a hydro-dynamical cluster simulation of a massive system ($M_{\text{virial}} = 2.1 \times 10^{15} M_{\odot}$ [14]; 1 Ms observation).

There are many different processes that can distribute the metals into the IGM, once they have been produced by stars. Gas-rich galaxies may lose their entire ISM by ram-pressure stripping in the densest parts of a cluster. Tidal tails caused by close galaxy-galaxy encounters is another enrichment mechanism that gains importance in the denser regions. Winds from galaxies, driven by strong starbursts or weaker galactic fountains caused by smaller fast-evolving massive star clusters may expel material from the galaxy, and is probably the most important enrichment process in cluster outskirts. Finally mergers of clusters with metal-enriched groups may also give rise to very localized abundance enhancements.

The strongest feedback process in clusters is the interaction of a SMBH residing in the core of the central giant elliptical galaxy at the heart of cool core clusters with the surrounding cluster gas. It has

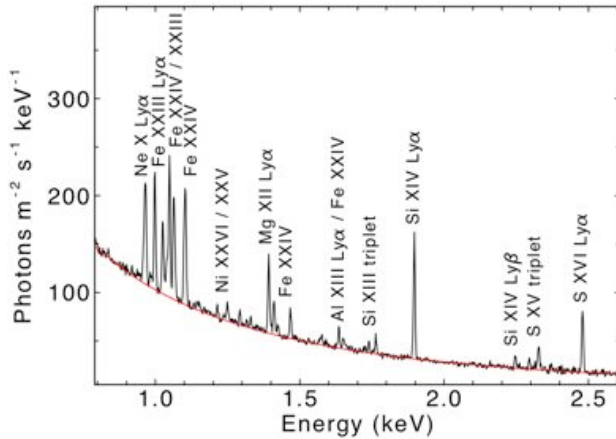


Figure 4: Close-up of a part of the spectrum of a bright cluster ($kT=2.5$ keV) as seen by CRIS in 100 ks. Note the large number of lines from different elements.

recently become clear that there is a delicate balance between the heating caused by AGN activity and the cooling of the gas due to X-ray radiation. Although the details of this process are not clear, it is known that it plays a crucial role in galaxy formation. *Xenia* will help solve this problem by studying metal circulation, heating and turbulence of the gas, processes that are intimately linked and form different aspects of the same feedback mechanism. Mapping at high spectral resolution is the key to understanding these

processes, both in the cooling cores as well as the outer regions of the cluster. In several dozen nearby clusters, the abundances of all elements: C, N, Ne, Mg, S, Ar, Ca, and Ni can be measured on at least an arcmin scale, and for the most abundant and important diagnostic elements (O, Si, Fe) down to the spatial resolution of *Xenia* (Figure 4). In addition, reliable abundances of Na, Al, P, Cl, K, Ti, Mn, Cr and Co integrated over the core can be obtained.

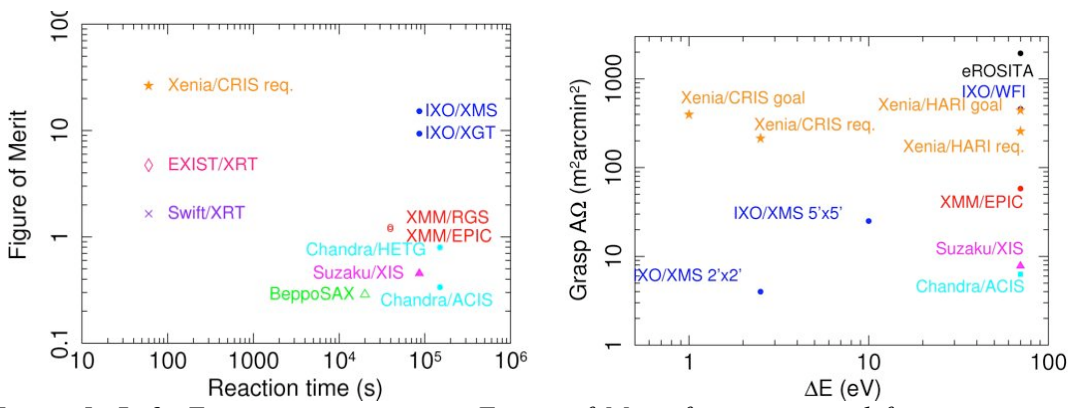


Figure 5: **Left:** Transient spectroscopy Figure of Merit for current and future instruments. **Right:** Grasp (at 0.5 keV) vs spectral resolution for the same instruments.

Groups of galaxies are ideal to study feedback processes that are relevant for *galaxy formation*. They show a higher entropy and lower density than the clusters, indicating that non-gravitational processes like pre-heating, radiative cooling, star formation, winds or AGN feedback have been important in shaping these objects. To nail down the importance of these processes, imaging spectroscopy is needed. While CCDs have delivered temperature and density maps for groups, they are poor in determining reliable abundance maps due to their low spectral resolution at the energies where the relatively cool group gas has most of its lines. *Xenia* will produce maps of T , n and abundances of key elements such as C, N, O, Ne and Fe for groups, which will allow us to trace the chemical and thermodynamic history of the groups. Apart from mapping nearby groups, lines from distant groups in filaments (out to $z \sim 0.15$) will also be detected in the deepest exposures, thereby identifying their role in the cosmic web. **Dynamics of clusters of galaxies:** Using the same cluster observations (deep exposures on both nearby and distant clusters), *Xenia* will determine *how homogeneous clusters are* by measuring localized density and temperature fluctuations in conjunction with systematic velocity fields and turbulence (line shapes) from our high-quality X-ray spectra; we will determine the *turbulent pressure* and its spatial scales. By finding substructures in the outer parts of clusters, we can determine *when the hydrostatic equilibrium conditions no longer apply*, and how that affects *DM mass estimates*. We may see *gas being ionized at accretion shocks* from the signatures of non-equilibrium ionization that will reveal the age of the plasma. *Particle acceleration at shocks* can be traced from satellite-to-resonance line ratios that are sensitive to the amount of non-thermal electrons in the plasma [15].

Why is Xenia unique? Figure 5 demonstrates the observational space addressed uniquely by the *Xenia* payload. We define a Figure of Merit (FoM) for transient spectroscopy as the S/N of a weak absorption line: $FoM = S/N = EW \sqrt{A_{eff} S_{GRB} / \Delta E}$, where EW is the equivalent width of the line, A_{eff} is the instrument effective area, S_{GRB} is the GRB fluence (flux integrated from the response time to 50 ks), and ΔE is the instrument energy resolution. FoM is plotted in Figure 5 (left panel) as a function of reaction time for a number of current and future instruments, assuming a 50 ks observation of a GRB afterglow with fluence 4×10^{-6} erg cm⁻². *Xenia* will open new observational windows in the Transient Universe: the combination of rapid S/C repointing (<60 s) with the *CRIS* spectral resolution and area make her a uniquely capable mission for high resolution spectroscopy of short-lived transients. Similarly, Figure 5 (right panel) shows that *CRIS* covers an unexplored window of high spectral resolution and high Grasp (light gathering power). *Xenia's* low inclination, low Earth orbit will result in low background, and her

large Grasp will enable deep imaging of the sky. Using these capabilities we firmly believe that our 5-year observing program will meet and exceed our core scientific goals.

The *Xenia* Transient Event Detector (TED)

The *Transient Event Detector* (TED) will monitor a >3 sr solid angle and will localize GRBs with a fluence greater than 10^{-6} erg cm $^{-2}$ (15-150 keV) with a positional uncertainty < 4 arcmin. The design has two identical imaging coded mask telescopes (Figure 6) tilted by 28° with respect to the optical axis of the HARI and CRIS. They have good efficiency between ~ 5 and 200 keV (2 mm thick CdZnTe detectors). A coded aperture instrument is the method of choice for the hard X-ray regime when both imaging and wide field coverage are necessary. It is well proven in space (*Swift*/BAT and *INTEGRAL*/IBIS are coded aperture instruments). Each camera is made up of 12 modules, each one being an assembly of 16×8 CZT crystals (size 10.8 \times 10.8 mm). Each crystal is a basic sensor made of 4×4 pixels, 2.7 mm size. The detector is surrounded on the bottom and sides with passive shields. The coded aperture mask is a 1 mm thick tungsten coded mask with a 4 mm cell size. It is designed to be a self-supporting pattern to allow X-ray transparency at the lowest energies. With a distance to the mask of 40.5 cm and a CZT pixel size of 2.7 mm, a location accuracy of 4 arcmin is achieved for sources detected with a S/N > 10 . Instrument requirements are given in Table 2 and the TED Mas-

Table 2: TED Instrument Requirements

Parameter	Requirement	Goal
Resolution at 100 keV	5 keV	3 keV
Field of View	3.15 sr	3.4 sr
Array size (pixels, one camera)	24,576	98,304
Energy range (keV)	5–200	3–200
On-axis Effective area, 20–50 keV (cm 2)	1500	1500
Angular resolution (FWHM)	34'	17'
Source location accuracy (10σ)	4'	2'
Min. count rate (background) [c/s]	2500	2500
Peak count rate [c/s]	7000	7000
S/W processing time	20s	10s
Continuum sensitivity	0.4	0.4

Table 3: TED Master Equipment List

Unit	CBE Mass (kg)	CBE Power (W)	TRL 2011
TED-1 detector	18.8	22.1	6
TED-1 mask	9.8		5
TED-1 shields	22.8		7
TED-2 detector	18.8	22.1	6
TED-2 mask	9.8		5
TED-2 shields	22.8		7
ICU	8.1	83.2	7
Total	110.9	127.4	
w/ margin	144	165	

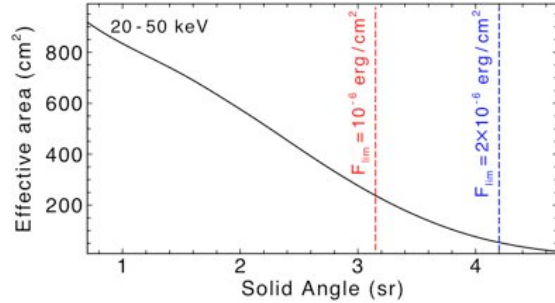


Figure 6: Effective area of the TED (2 units) vs solid angle with limiting burst fluences for two different FOV limits.

ter Equipment List is given in Table 3.

Signal Detection: Hard X-rays are detected by CZT detectors and digitized by front-end electronics. A single computer serving both TED telescopes provides the processing for trigger, validation and positioning of gamma-ray transient events and controls the S/C interface and TM/TC. The instrument concept has been well tested by *Swift*/BAT [16].

The Xenia Cryogenic Imaging Spectrometer (CRIS)

The *Cryogenic Imaging Spectrometer* (CRIS; right) makes full use of recent developments in detector and mirror technology. Arrays of X-ray calorimeters now allow for imaging in the X-ray band with a few eV energy resolution (see appendix). This resolution is required to detect weak emission and absorption lines linked to the WHIM. A large FoV is achieved by using very short focal length (1.2 m) foil optics. The telescope uses four reflections for the outer shells to obtain a large effective area while retaining low grazing angles (see appendix). The interior shells use two reflections. CRIS will image with excellent spectral resolution over an energy range between 0.2 and 2.2 keV where the most abundant highly ionized and red-

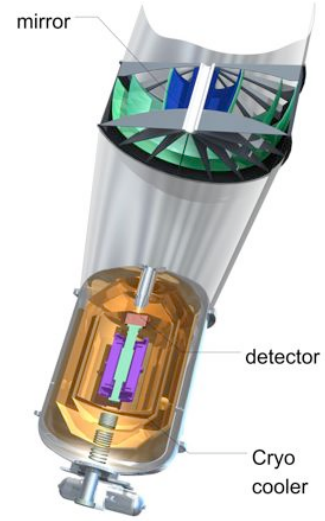


Table 4: CRIS Instrument Requirements

Parameter	Requirement	Goal
Resolution at 0.5 keV	2.5 eV	1 eV
Field of View	0.9°×0.9°	1°×1°
Array size [pixels]	2000	2176
Energy range [keV]	0.2 – 2.2	0.1 – 3.0
Effective area @ 0.6 keV	1000 cm ²	1300 cm ²
grasp@0.6 keV [cm ² deg ²]	400	500
Angular resolution (HPD)	4 arcmin	2.5 arcmin
Peak count rate [c/s]	10,000	15,000

Table 5: CRIS Master Equipment List

Unit	CBE Mass [kg]	CBE Power [W]	TRL 2011
Mirror	107	100	4
TES detector	42	200	4
Cooling	254	540	5
Structure	39	0	> 6
Total	442	840	
w/ margin	575	1092	

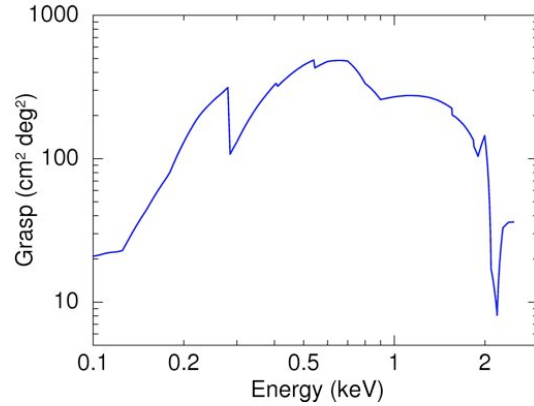


Figure 7: CRIS Grasp ($A\Omega$) taking into account mirrors, filters, and detectors.

shifted species will emit or absorb. Instrument requirements are given in Table 4; the top-level Master Equipment List is given in Table 5.

CRIS is clearly the most challenging instrumental part of the *Xenia* mission and we describe the two technical drivers in more detail in the appendix. On the other hand, cryogenic detectors and the full

cryocooling systems have made major advances over the last year and similar detectors will be flown on the *Astro-H* mission. The detector and its cooling will be developed by a consortium including NIST, NASA/GSFC, JAXA/ISAS, INAF/IASF, TMU, and NL/SRON. **Signal detection:** Onboard data processing is required to obtain the optimal resolution using optimal filtering. This technology has been developed for *Suzaku*; it will be employed for *ASTRO-H* as well and needs to be scaled to the larger array of *CRIS*.

The *Xenia* High Angular Resolution Imager (HARI)

The *High Angular Resolution Imager* (HARI) is a wide field X-ray telescope combining wide-angle mirrors with a state-of-the-art Si-based focal plane array (CCDs or CMOS detectors). The combination of good angular resolution, low background, and a very wide field of view is required for studies of galaxy clusters and the WHIM. The tele-

scope design uses polynomial approximations to a Wolter I to reduce off-axis aberrations and provide excellent imaging performance over a wide field of view, allowing *Xenia* to measure properties of the cluster gas beyond the virial radius. Instrument requirements are given in Table 6 and the Master Equipment List is given in Table 7. These requirements are all achievable at the current state-of-the-art. **Signal detection:** HARI will require short effective frame times to prevent pile-up from observations of

Table 6: HARI instrument requirements

Parameter	Requirement	Goal
Resolution at 0.5 keV	80 eV	70 eV
Resolution at 5.9 keV	150 eV	130 eV
Field of View (diameter)	1.4°	1.5°
Energy range [keV]	0.3 – 5.0	0.2 – 10.0
Effective area @ 1 keV	530 cm ²	1000 cm ²
Effective area @ 6 keV	25 cm ²	100 cm ²
Angular resolution (HPD)	15 arcsec	10 arcsec
Time resolution	0.5 s	0.1 s
Peak count rate [c/s]	10,000	30,000
Instrumental background @ 1 keV [cts/cm ² /s/keV]	1.5 x 10 ⁻³	6 x 10 ⁻⁴

bright GRB afterglows. Data frames will be processed to identify X-ray events on the basis of their charge distribution across adjacent pixels, thus providing highly efficient rejection of cosmic rays and allowing significant data compression. This technology is well understood and has been implemented in either hardware or software in *ASCA/SIS*, *Chandra/ACIS XMM-Newton/EPIC*, and the *Swift/XRT*.

Table 7: HARI Master Equipment List

Unit	CBE Mass (kg)	CBE Power (W)	TRL 2011
Mirror	155	21	5
Tube	87	46	6
Camera	17	11	6
E-box	29	32	6
Misc	7	5	N/A
Total	295	115	
w/ margin	384	150	

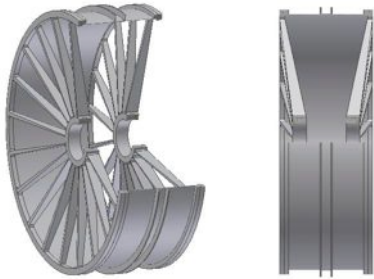


Figure 8: Wide-field X-ray optics design.

The *Xenia* Spacecraft Concept

Xenia uses a 3-axis stabilized spacecraft compatible with the Falcon 9 launcher, which may be launched from Cape Canaveral Air Force Station or Omelek Island at the Reagan Test Site. The spacecraft concept (Figure 9) is based on proven spacecraft systems and subsystems. The spacecraft is capable of fast, autonomous repointing after GRB detections.

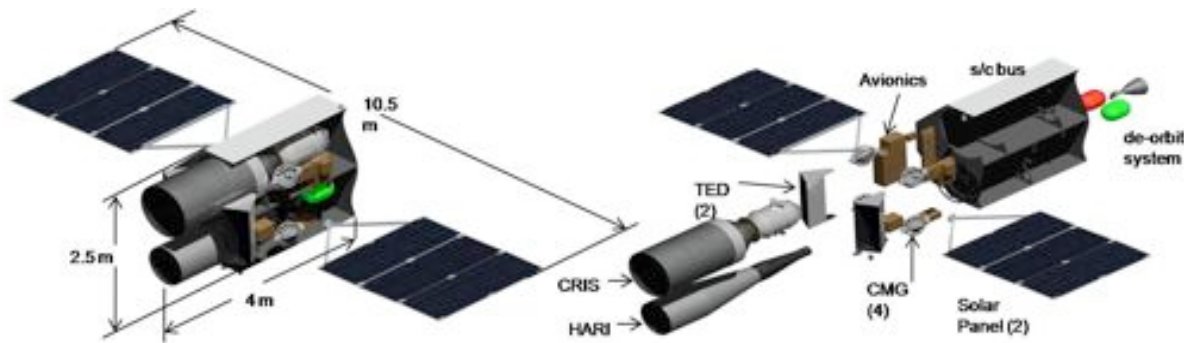


Figure 9: *Xenia Spacecraft Concept*

The NASA/MSFC's Advanced Concepts Office developed the spacecraft concept specifically for *Xenia*. Table 8 shows spacecraft key performance requirements. Table 9 shows the total spacecraft mass broken down by primary subsystems.

Table8: *Xenia Spacecraft and Mission Summary*

Requirement	Summary
Orbit	600 km LEO; Inclination $\leq 10^\circ$
Pointing	3-axis stabilized w/ 45° sun-avoidance; Pointing knowledge < 2 arcsec, accuracy < 2 arcmin
Rapid Slew	60° in 60 sec, autonomous (on-board decision and slew planning, as on <i>Swift</i>)
Lifetime	Spacecraft: 5 Years; Orbit: 10 years
Mass	2637 kg (incl. 30% mass growth allowance)
Power	2027W available at end-of-life (incl. 30% margin); Includes battery charging and peak power
Telemetry	Ku Band omni-directional; 3.8 Mbps orbital avg via TDRSS; 4 kbps available for uplink and rapid downlink

The *Xenia* spacecraft concept does not require any new technology. The high-accuracy, rapid repointing capability benefits from the recently space-qualified Ball Aerospace Worldview control moment gyros (CMGs) and 2 sets of star trackers that have both wide and narrow FoV.

Table9: *Xenia Spacecraft Mass Properties Summary*

Weight Breakdown Structure			Qty	Unit Mass (kg)	Total Mass (kg)
1.0	Structure				399
2.0	Propulsion				16
3.0	Power				170
4.0	Avionics / Control				426
5.0	Thermal Control				33
6.0	Growth				313
Dry Mass					1357
7.0	Non-Cargo				6
8.0	Science Instruments				1138
	8.1	CRIS	1	575	575
	8.2	HARI	1	384	384
	8.3	TED	2	72	144
	8.4	Instrument Cabling	1	35	35
Inert Mass					1144
Total Less Propellant					2501
9.0	Propellant				137
Gross Mass					2638

Cost Estimates

The mission funding profile is given in Table 10 in FY 2010 dollars. The total cost estimate, including contingency, is \$904.4M. *Xenia falls well within the RFI range at the upper medium, lower large mission category (with/without international contributions).*

The spacecraft costs (Table 10) were estimated by MSFC using the NAFCOM cost model and cost data from *COBE*, *Swift* and *GLAST* (the cost of the Falcon 9 launch vehicle was taken from data at <http://www.spaceref.com/>).

CRIS cost estimates have been based on recent cost estimates for *IXO* and *Athena*. *CRIS* includes three major subsystems: the cryocooler, the optics and the instrument electronics plus detector. For the cryocooler, the design is based on *Astro-H* and does not require any new technology; it will be built in Japan (JAXA/ISAS). Optics production is also in Japan (Nagoya University). The management and systems engineering and one of the three detector subsystems (read-out) will be done by SRON, the detector by GSFC, and the anti-coincidence detector by INAF. **HARI** costs are based on inflated and scaled actual costs for the *Swift/XRT* (launched in 2004) and the *JANUS* XRFM instrument (in Phase A). *HARI* includes three major subsystems: optics, focal plane array, and electronics. The optics design has been demonstrated and is straightforwardly achievable using diamond-turned mandrels and replicated mirrors. The focal plane array is now fairly standard technology, as are the instrument electronics. We baselined CMOS detectors for budgetary purposes, but CCDs are also possible; a selection will be made in Phase A. Costs were estimated by a grass-roots approach based on actual costs for the *Swift/XRT* and projected costs for the *JANUS/XRFM*. **TED** costs were based on inflated and scaled actual costs for the *INTEGRAL* IBIS instrument (launched in 2002) and the *SVOM* ECLAIRs instrument (in Phase A). *TED* has three major subsystems: detectors, masks and digital electronics. The design of the detectors is very similar to the *Swift-BAT* and *IBIS* and is based on 24 CZT modules to be assembled in two identical detection planes. We assume that the detector Front-End-Electronics, including the module Digital Front-end, will be provided by the US while the CZT parts, the mechanical assembly parts and the on-board processing electronics will be provided by Italy (heritage: *IBIS*, *AGILE*).

The Mission Ops include a 1.5 year startup effort overlapping Phases D and E and five-years of routine operations in Phase E. Included in this total are Mission and Science Ops, Facilities, and funding for the Instrument Teams, plus \$25M to Guest Investigators and \$5M to EPO. They include no contingency on GI and EPO programs, 20% contingency on instrument team funding, and 30% contingency on other costs. The international partners contribute ~20% of the Mission Ops costs.

Table10: Mission Funding Profile in FY2010 millions of dollars

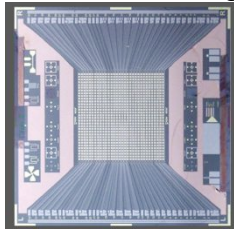
	Phase A	Phase B	Phase C/D	Phase E		
	2012	2013	2014-16	2018-23	Total	w/ margin
S/C and LV	9.4	8.2	338.3	0	375.9	488.7
Instruments	17.2	65.7	274.1	0	360.5	459.9
Mission Ops			3.6	76.3	79.9	91.7
Grand Total					1040.3	
International Contributions						238.4
Total from NASA						801.9

Appendix

Xenia Technology Driver 1: CRIS Detector

The detector is an imaging X-ray spectrometer based on a pixel array of microcalorimeters. Each pixel consists of an absorber (e.g. Bi/Cu) of which the temperature is measured by a normal-to-superconducting phase transition thermometer with a critical temperature $T_c \approx 100$ mK, generally called a Transition Edge Sensor (TES). The absorber-thermometer combination is weakly coupled to the 50 mK base temperature of the cryostat. The basic properties of these detectors have been proven and large arrays are under development for different applications (*Xenia*, *IXO*, *micro-X* (rocket experiment to be launched in 2011)).

For the cooling to sub-K temperatures a cryogen-free system will be used. Many options exist using a combination of coolers for different stages at 100 K, 20 K, a few K and sub-K (Stirling coolers, Joule-Thomson coolers, adiabatic demagnetization refrigerators, sorption coolers, pulse tube coolers or dilution fridge closed cycle coolers). The challenge is to optimize the efficiency of the cooling system. We have selected a system based on the cooler design for the *Astro-H* mission and scoped it to include redundancy at the level of each mechanical cooler. Following the *Astro-H* mission this design will have a high TRL (> 6).



micro-machined 32 x 32 array (SRON, 2005)

The basic principle of the detector has been demonstrated in Europe and in the US with resolutions < 3 eV (Figure 1) while also meeting the other requirements (such as count rate capability). To cope with the very high count rates for GRBs a small section of the detector will be located out-of-focus, lowering the count rates per pixel by a factor of 10 or more (at the expense of blurring the image, which is of no concern for these strong point sources). Production technology to make such arrays is well in hand.

The most critical part of the detector is to read out large arrays while keeping the electrical connections limited to minimize heat conduction. Two different technologies have been demonstrated on a small scale but need to be scaled up to the full array (2176 pixels or 68 channels of 32 pixels). Time Domain Multiplexing has been demonstrated for an array of 2 x 8 pixels (GSFC/NIST; Figure 1) and is currently being scaled up to columns of 32 pixels. The principle of Frequency Domain Multiplexing has been demonstrated experimentally (SRON).

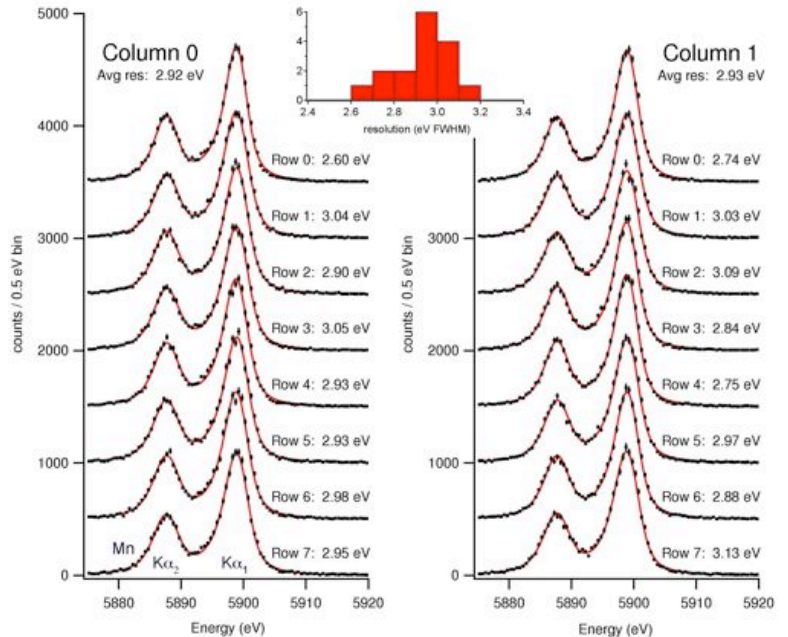


Figure 1: Results for a multiplexed 2x8 pixel array (NIST/GSFC, 2008). Each spectrum is from a different pixel/channel on the array; resolution varies from 2.60 to 3.13 eV across the array.

Xenia Technology Driver 2: CRIS Mirrors

A low mass, large collecting area mirror will be made using thin foil technology originally developed for the Japanese satellites *ASCA* and *Suzaku*. In these segmented mirrors (four 90° quadrants) thin foils will be accurately mounted in a rigid support structure. The modest angular resolution of this approach is fully consistent with the mission requirements.

The basic principle of X-ray optics makes use of high reflectivity at grazing incidence angles. Using mirrors made of thin foils coated with gold we have demonstrated that angular resolutions of about 1.5 arcmin are feasible for 4-6 m focal length (*ASCA* 1993, *Suzaku* 2005, *Astro-H* to be launched in 2013). In order to increase the effective area while still keeping graze angles small, the outer shells for CRIS will employ four reflections; the reduction in throughput caused by these additional reflections is more than compensated by the larger reflectivity due to the smaller incident angle per reflection (Figure 2). To optimize the effective area at low energies the foils will employ carbon overcoated with Pt for the inner mirrors and with Ni for the outer mirrors. The use of 4-fold reflections is a novel technique not yet implemented for X-ray astronomy. However, the basic technology is well understood and a program to bring this to TRL6 is underway at Nagoya University. Within the next two years, a medium-scale engineering model with several tens of shells including both 2- and 4-fold reflectors with diameter larger than 40 cm will be fabricated and tested with X-rays to establish the whole process needed to make Xenia optics.

Optical tests carried out at Nagoya University to confirm this principle show a resolution of 4.1 arcmin (Figure 3), which is consistent with our expectations for a 4 arcmin X-ray mirror. Integration of the 137 shells in its support structure is well proven technology (*ASCA*, *Suzaku*) and the required accuracies ($< 7\text{-}8\text{ }\mu\text{m}$) have been regularly demonstrated on those programs.

References

- [1] Gonzales et al. 2007, *ApJ*, 666, 147; [2] Paerels et al. 2008, arXiv:0810.1754; [3] Gao & Theuns 2007, *Science*, 317, 1527; [4] Branchini et al. 2009, *ApJ*, 697, 328; [5] Borgani et al. 2004, *MNRAS*, 348, 1078; [6] Viel et al. 2004, *MNRAS*, 354, 684; [7] Cen & Ostriker 2006, *ApJ*, 650, 560; [8] Danforth & Shull 2008, *ApJ*, 679, 194; [9] Cen & Ostriker 1999, *ApJ*, 519, L109; [10] Werner et al. 2008, *A&A*, 482, L29; [11] Dolag et al. 2006, *MNRAS*, 370, 656; [12] Bregman 2007, *ARAA*, 45, 221; [13] Conroy & Ostriker 2008, *ApJ*, 681, 151; [14] Roncarelli et al. 2006, *MNRAS*, 373, 1339; [15] Gabriel & Phillips 1979, *MNRAS*, 189, 319; [16] Barthelmy et al. 2005, *Space Sci. Rev.*, 120, 143

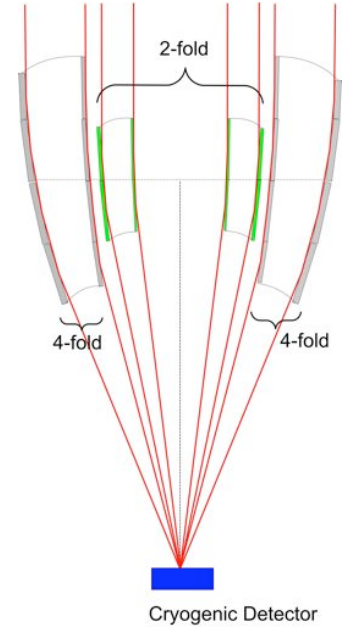


Figure 2: Schematic of the CRIS X-ray optics design employing 2-fold reflections for the inner shells and 4-fold reflections for the outer shells.

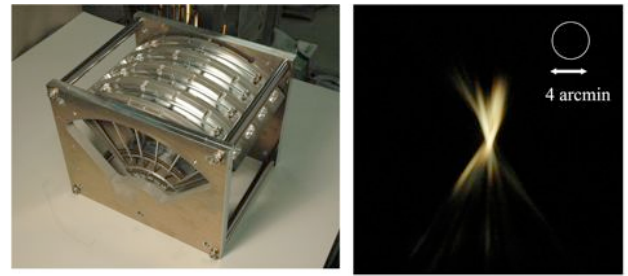


Figure 3: **Left:** Foil mirror housing (one quadrant) and interface adapter for X-ray tests. **Right:** PSF measured in optical test of mirrors with 4 reflections.